OPTOELECTRONICS AND ADVANCED MATERIALS – RAPID COMMUNICATIONS Vol. 14, No. 7-8, July-August 2020, p. 302 - 305

Reflective grating embedded between two dielectric slabs under second Bragg mounting

JIMIN FANG, BO WANG*, CHEN FU, KUNHUA WEN, ZIMING MENG, QU WANG, ZHAOGANG NIE, XIANGJUN XING, LI CHEN, LIANG LEI, JINYUN ZHOU
School of Physics and Optoelectronic Engineering, Guangdong University of Technology, Guangzhou 510006, China

A novel design of reflective single-port polarization-independent grating with a metal mirror, a connection layer and a covering layer under second Bragg mounting is reported in this paper. A better grating structure by rigorous coupled-wave method can be obtained. The grating parameters are optimized for high-efficiency output. The optimization results show that in the wavelength range of 1546-1554 nm or the incident angle is between 38.0-39.3°, the -2nd order of the grating has a good high-efficiency output effect, and the efficiency can reach more than 90%, which will be a good application in the field of laser.

(Received November 16, 2019; accepted August 18, 2020)

Keywords: Single-port output, Reflective grating, Under second Bragg mounting

1. Introduction

With the second Bragg condition, the gratings can fulfill some great beam-splitting functions. The beam splitter [1-10] is a device for dividing an incident beam into many beams into different directions, which can be used in laser micro-nano fabrications [11-14], grating couplers [15-18], reflectors [19-23], optical storages [24,25]. Metasurfaces elements can be applied in wide-band/angle blazing operation [26], full color generation [27], nanophotonics with multipurpose functionalities [28], phase resonance tuning and multi-band absorption [29], beam manipulating [30,31], and reversible multi-stage switching of phase-change [32]. Recently, the single-port high-efficiency gratings can attract more attention in high-power output. Wang et al. proposed a single-port grating with an incident wavelength of 1550 nm [33]. A reflective grating with a connection layer was proposed under the Bragg mounting [34]. The diffraction efficiencies higher than 95% about 1550 nm wavelength for both TE and TM polarizations can be obtained. To our knowledge, reflective single-port polarization-independent grating with a metal mirror, a connection layer and a covering layer under second Bragg mounting has not been reported before.

In this paper, the -2nd order polarization-independent single-port reflective grating with an incident wavelength of 1550 nm is proposed. Such a grating is analyzed and designed by using rigorous coupled-wave analysis (RCWA) [35]. Based on the vector analysis of grating, RCWA method is used to solve the Maxwell equation, and the diffraction efficiency of TE and TM polarization states may be obtained. By optimization, the efficiencies of 96.60% and 96.33% can be obtained for TE and TM polarizations in -2nd order.

2. High-efficiency polarization independence

The structure of the reflective single-port grating is shown in Fig. 1. The grating is under second Bragg mounting with the incident angle of $\theta=\sin^{-1}(\lambda/n_1/d)$ at a wavelength of 1550 nm. The top of the grating is covering layer. Its medium is fused silica [36-39]. The depth of the covering layer is h_1. The width of grating ridge is b with the depth of h_2. The grating period is d and the grating duty cycle is f. The covering layer and the grating layer are composed of fused silica with refractive index of n_2=1.45 [40, 41]. The grating groove is air with refractive index of n_1 =1.0. The thickness of the connecting layer is h_3. Its medium is also fused silica. The metal mirror is Ag with refractive index of n_m =0.469-i*9.32. By theoretical calculation using RCWA, we set the duty cycle to f =0.64, the period d=2484 nm, and h_3= h_m=0.1 μm.

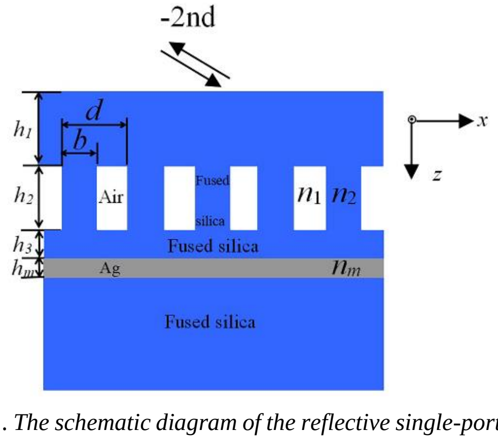

Fig. 1. The schematic diagram of the reflective single-port grating at wavelength of 1550 nm with duty cycle of 0.64 under second Bragg mounting (color online)

The grating groove depth and the thickness of covering layer need to be optimized according to the known parameters. Fig. 2 shows the reflective efficiencies in the -2nd order versus grating groove depth and the thickness of covering layer for TE and TM polarizations at wavelength of 1550 nm with duty cycle of 0.64 under second Bragg mounting. In the case of h_1=0.48 μm and h_2=1.92 μm, the efficiency of the -2nd order is 96.60% for TE polarization, and the efficiency of -2nd order under TM polarization is 96.33%.

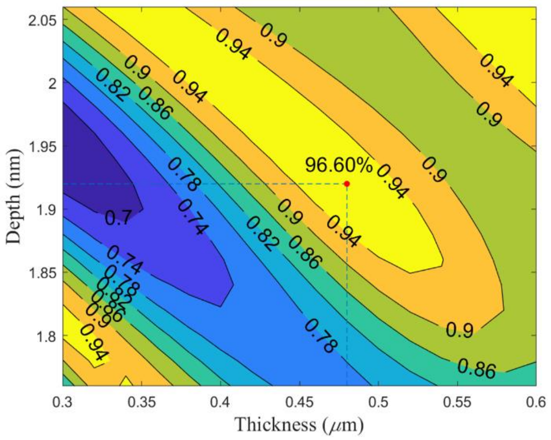

(a)

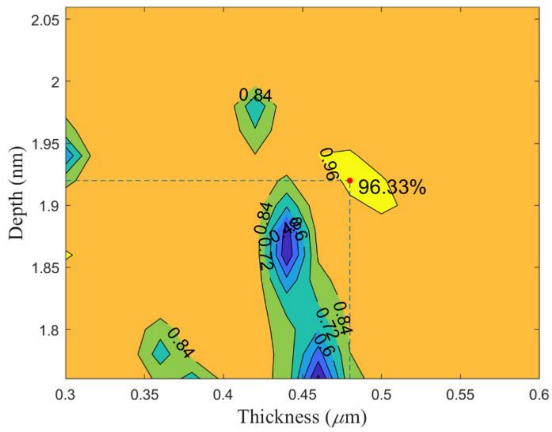

(b)

Fig. 2. Reflective efficiencies in the -2nd order versus grating groove depth and the thickness of covering layer for TE and TM polarizations at wavelength of 1550 nm with duty cycle of 0.64 under second Bragg mounting: (a) TE polarization and (b) TM polarization (color online)

Fig. 3 shows the field distribution normalization of a single-port reflective grating showing the energy distribution of the grating in the grating region. One can see the propagating process from the Fig. 3.

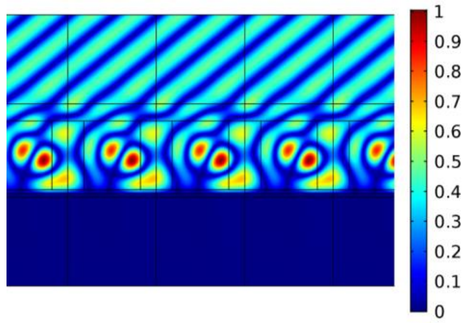

(a)

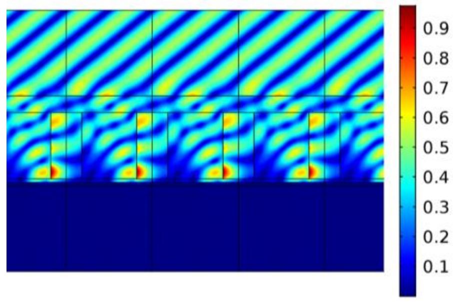

(b)

Fig. 3. Normalized field magnitude distribution with optimized reflective beam splitter near second Bragg mounting: (a) TE polarization and (b) TM polarization (color online)

3. Analysis and discussions

When the incident wavelength and angle deviate from the optimized result, the performance of the grating is affected. Therefore, we need to further consider the influence of the incident angle on the reflection efficiency of the grating. Fig. 4 shows the efficiency corresponding to the incident wavelength with duty cycle of 0.64 under second Bragg mounting. The -2nd order efficiency of the grating is greater than 90% under both polarizations when the wavelength is between 1541-1557 nm.

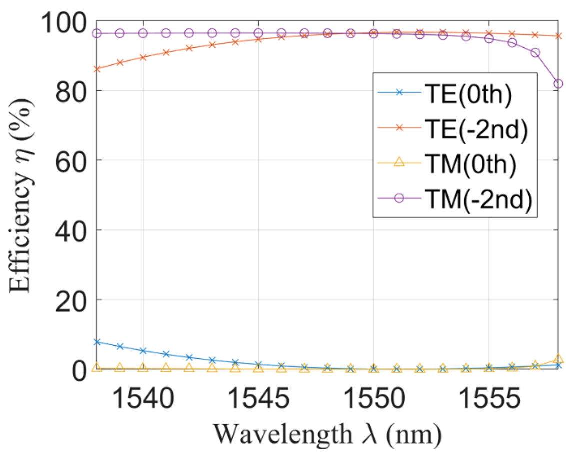

Fig. 4. The efficiency corresponding to the incident wavelength with duty cycle of 0.64 under second Bragg mounting (color online)

Fig. 5 shows the relationship between the reflection efficiency of the grating and the angle of mounting under optimized grating parameters. In the case where the efficiency at both polarizations is greater than 95%, the angle range is 38.0-39.3°. The efficiencies of 96.60% and 96.33% can be obtained for TE and TM polarizations when the angle is 38.6°.

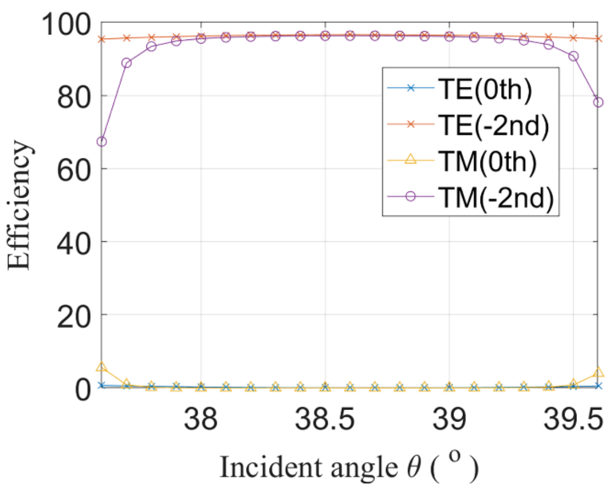

Fig. 5. The diffraction efficiency corresponding to the incident second Bragg angle (color online)

In the process of multilayer grating fabrication, grating etching is very important for grating characteristics. Therefore, the period and duty cycle of the grating will change compared to the ideal state of the design. The period and duty cycle of the grating need to be discussed. Fig. 6 shows the relationship between the duty cycle of the grating and the reflection efficiency. When the duty cycle of the grating is 0.628-0.672, the efficiency of the -2nd order under the two polarizations is greater than 90%.

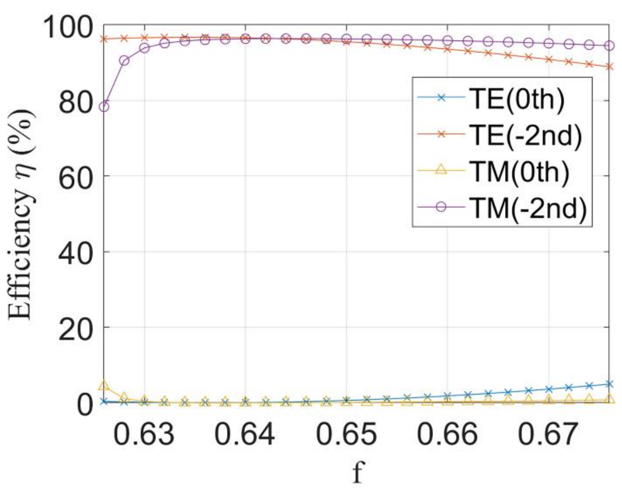

Fig. 6. The diffraction efficiency corresponding to the duty cycle under second Bragg mounting (color online)

As a result of the optimization design of single-port grating with an incident wavelength of 1550 nm under an incident second Bragg angle of 38.6°, some high-efficiency performances are also obtained based on different period under the duty cycle of 0.64. Fig. 7 shows the efficiency corresponding to the period with duty cycle of 0.64 under second Bragg mounting. The efficiencies at both polarizations is greater than 90% when the period is 2476-2492 nm.

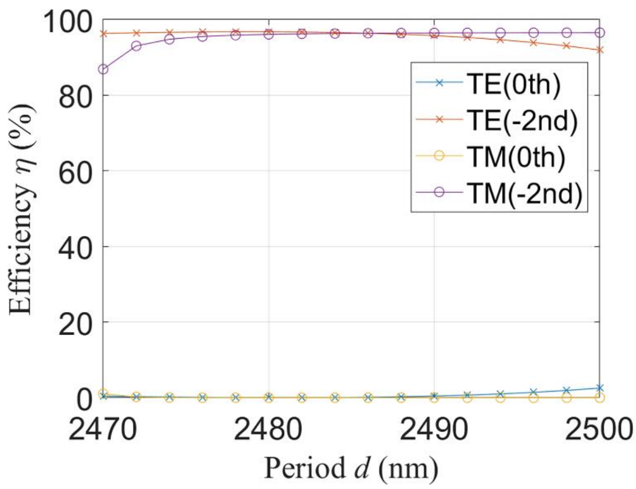

Fig. 7. The efficiency corresponding to the period with duty cycle of 0.64 under second Bragg mounting (color online)

4. Conclusion

In this paper, we propose and design a reflective single-port polarization-independent grating with a metal mirror, a connection layer and a covering layer under second Bragg mounting by employing rigorous numerical optimization method. The duty cycle is 0.64 and the period is 2484 nm. The efficiency is greater than 95% under two polarizations can be obtained when the thickness of the covering layer is 0.48 μm and the depth of grating layer is 1.92 μm. The polarization-independent grating shows high efficiency with long period under second Bragg mounting.

Acknowledgements

This work is supported by the Science and Technology Program of Guangzhou (202002030284, 202007010001).

References

[1] H. Huang, T. Zhai, Q. Song, X. Yin, Opt. Commun. **434**, 28 (2019).
[2] H.-C. Yuan, X.-X. Xu, Y.-J. Xu, Optik **172**, 1034

(2018).
[3] Q. Tao, J. Wang, C. Hu, Optoelectron. Adv. Mat. **13**(1), 1 (2019).
[4] E. Rafiee, F. Emami, R. Negahdari, Optik **172,** 234 (2018).
[5] H. Yang, K. Ou, G. Gao, X. Shang, Y. Liu, Y. Deng, Opt. Commun. **443**, 104 (2019).
[6] A. Fedaouche, H. A. Badaoui, M. Abri, Optik **157**, 1300 (2018).
[7] Y.-Y. Fei, X.-D. Meng, M. Gao, Z. Ma, H. Wang, Optik **170**, 368 (2018).
[8] M. A. Butt, S. N. Khonina, N. L. Kazanskiy, Laser Phys. **29**(4), 046207 (2019).
[9] M. A. Butt, S. N. Khonina, N. L. Kazanskiy, Laser Phys. **28**(11), 116202 (2018).
[10] T. Sun, Z. Zhou, W. Zhang, Laser Phys. **28**(12), 125601 (2018).
[11] L. Derbali, M. Dkhili, S. Zargouni, M. Ouadhour, R. Riahi, H. Ezzaouia, Superlattices Microstruct. **123**, 427 (2018).
[12] Z.-Y. Hu, Y.-L. Sun, J.-G. Hua, IEEE Photon. Technol. Lett. **31**(2), 133 (2019).
[13] Z.-H. Yan, S. Zhou, Mod. Phys. Lett. B **32**(19), 1850214 (2018).
[14] S. Liu, H. Wu, Y. Shi, B. Qiu, R. Xiao, M. Chen, H. Xue, L. Hao, Y. Zhao, J. Lu, X. Chen, IEEE Photon. Technol. Lett. **31**(10), 751 (2019).
[15] Y. Chen, L.-A. Bian, P. Liu, G. Li, Y. Xie, Superlattices Microstruct. **124**, 185 (2018).
[16] T. Watanabe, Y. Fedoryshyn, J. Leuthold, IEEE Photon. J. **11**(4), 7904709 (2019).
[17] C. Li, K. Zhang, Y. Zhang, Y. Cheng, W. Kong, Opt. Commun. **437**, 271 (2019).
[18] Yang, T. Wang, J. Zheng, Laser Phys. Lett. **16**(2), 025104 (2019).
[19] Fang, S. Han, J. Xie, Optoelectron. Adv. Mat. **13**(3), 175 (2019).
[20] S. K. Evran, O. Coskun, Optoelectron. Adv. Mat. **13**(1), 78 (2019).
[21] G. Ju, S. Lee, B. H. Na, Optoelectron. Adv. Mat. **12**(3), 137 (2018).
[22] T. Bi, C. Wang, J. Zhou, Opt. Eng. **57**(5), 051505 (2018).
[23] K. Wu, H. Fang, L. Lan, Opt. Eng. **58**(2), 025106 (2019).
[24] F. Xu, J. Zhu, S. Fan, Y. Qi, Mod. Phys. Lett. B **33**(20), 1950226 (2019).
[25] L. Zheng, Y. Hu, J. Xu, Optoelectron. Adv. Mat. **12**(9), 584 (2018).
[26] O. Hemmatyar, M. A. Abbassi, B. Rahmani, M. Memarian, K. Mehrany, IEEE Trans. Antennas Propag. DOI: 10.1109/TAP.2020.3001458 (2020).
[27] O. Hemmatyar, S. Abdollahramezani, Y. Kiarashinejad, M. Zandehshahvar, A. Adibi, Nanoscale **11**(44), 21266 (2019).
[28] S. Abdollahramezani, O. Hemmatyar, H. Taghinejad, A. Krasnok, Y. Kiarashinejad, M. Zandehshahvar, A. Alù, A. Adibi, Nanophotonics **9**(5), 1189 (2020).
[29] O. Hemmatyar, B. Rahmani, A. Bagheri, A. Khavasi, IEEE J. Quantum Electron. **53**(5), 7000810 (2017).
[30] S. Abdollahramezani, K. Arik, S. Farajollahi, A. Khavasi, Z. Kavehvash, Opt. Lett. **40**(22), 5383 (2015).
[31] K. Arik, O. Hemmatyar, Z. Kavehvash, Plasmonics **15**(3), 639 (2020).
[32] H. Taghinejad, S. Abdollahramezani, A. A. Eftekhar, T. Fan, A. H. Hosseinnia, O. Hemmatyar, A. E. Dorche, A. Gallmon, A. Adibi, arXiv:2003.04097v2 (2020).
[33] S. Wang, C. Zhou, Y. Zhang, H. Ru, Appl. Opt. **45**(12), 2567 (2006).
[34] B. Wang, L. Lei, L. Chen, J. Zhou, Opt. Commun. **285**(21), 4599 (2012).
[35] M. G. Moharam, E. B. Grann, D. A. Pommet, T. K. Gaylord, J. Opt. Soc. Am. A **12**(5), 1068 (1995).
[36] Y. Shu, Optik **178**, 544 (2019).
[37] W. Liao, X. Nie, Z. Liu, X. Nie, W. Wan, Optik **179**, 957 (2019).
[38] E. V. Vasilyev, S. A. Shlenov, V. P. Kandidov, Laser Phys. Lett. **15**(11), 115402 (2018).
[39] X. Gao, R. Qiu, K. Yao, Laser Phys. Lett. **15**(10), 106001 (2018).
[40] Q. Cong, G. Yuan, C. Zhang, B. Guo, IEEE Photon. Technol. Lett. **30**(8), 724 (2018).
[41] M. Fajkus, M. Novak, J. Nedoma, Optoelectron. Adv. Mat. **13**(3), 168 (2019).

*Corresponding author: wangb_wsx@yeah.net